

The Deconfinement Phase Transition in Asymmetric Matter

Horst Müller*

Physics Department and Nuclear Theory Center

Indiana University, Bloomington, Indiana 47405

(September 16, 2018)

Abstract

We study the phase transition of asymmetric hadronic matter to a quark-gluon plasma within the framework of a simple two-phase model. The analysis is performed in a system with two conserved charges (baryon number and isospin) using the stability conditions on the free energy, the conservation laws and Gibbs' criteria for phase equilibrium. The EOS is obtained in a separate description for the hadronic phase and for the quark-gluon plasma. For the hadrons, a relativistic mean-field model calibrated to the properties of nuclear matter is used, and a bag-model type EOS is used for the quarks and gluons. The model is applied to the deconfinement phase transition that may occur in matter created in ultra-relativistic collisions of heavy ions. Based on the two-dimensional coexistence surface (binodal), various phase separation scenarios and the Maxwell construction through the mixed phase are discussed. In the framework of the two-phase model the phase transition in asymmetric matter is continuous (second-order by Ehrenfest's definition) in contrast to the discontinuous (first-order) transition of symmetric systems.

*Present address: *TRIUMF, 4004 Wesbrook Mall, Vancouver, B.C. Canada V6T 2A3*

I. INTRODUCTION

The determination of the phase structure of strongly interacting matter is one of the major challenges in theory and experiment. In our contribution we study the phase transition from hadrons to a quark-gluon plasma in asymmetric matter. Based on a two-phase model we describe new qualitative features that arise as a function of the isospin and that may be relevant for the phenomenological description of highly energetic heavy-ion collisions.

The creation of the quark-gluon plasma and the elucidation of its properties is the fundamental goal in relativistic heavy-ion physics. Although experiments at the Brookhaven AGS and at the CERN SPS have provided evidence that in highly energetic collisions an intermediate state is formed which is characterized by very high energy densities [1], it is not clear if this new phase of matter has actually been reached (for a recent review, see [2]).

On the theoretical side the determination of the equation of state (EOS) of strongly interacting matter at high temperatures and densities is a major problem in QCD. One of the most important issues here is revealing the phase diagram of matter and the nature of the transition. Most reliable results come from lattice calculations for systems at zero baryon density (for an updated status report see [4]). These calculations clearly indicate a first-order transition for pure $SU(3)$ gauge theories [3]. When dynamical quarks are added the situation is less transparent. The nature of the transition not only depends on the number of flavors but also on their masses [5,6], particularly on the mass of the strange quark. For example, three light flavors show a first-order transition that is absent for larger masses [5]. Despite the need of corresponding information in applications to heavy-ion collisions, lattice calculations at finite baryon density presently remain at an early stage without a definite conclusion [4].

To the best of our knowledge, there are no lattice calculations available for asymmetric systems, *i.e.*, systems at finite baryon density and with nonzero isospin. However, it has been demonstrated in case of the liquid-gas phase transition of nuclear matter that asymmetric systems have qualitatively different properties than symmetric systems [7–9]. In particular,

the transition in an asymmetric system is *continuous* and of second order according to Ehrenfest's definition, in contrast to the discontinuous, first-order transition in symmetric systems. The goal of the present work is to extend these studies to the deconfinement phase transition of asymmetric matter. Since lattice calculations cannot provide the required information at present, we resort to a separate description of the hadronic and the quark-gluon phase. This approach is not new and was previously employed to investigate the existence of quark cores in neutron stars [10,11]. Although such a formulation oversimplifies the full complexity of the problem, it is useful for providing a first orientation to the new features that arise when a system with two conserved charges, *i.e.*, baryon number and isospin, undergoes a transition.

The EOS for the quark-gluon phase is based on a simple "bag model", where the thermodynamic potential is modeled as a sum of a perturbative contribution and a nonperturbative part which is represented by the bag constant. Along these lines we adopt a model which is based on two massless flavors and which includes the first-order correction in the strong coupling constant α_s [11,12].

The hadronic EOS is generated in a relativistic mean-field approach involving the interaction of Dirac nucleons with isoscalar scalar and vector meson fields and with isovector ρ meson and pion fields [13,14]. The central object in this approach is an energy functional of the meson mean fields, which, in principle, can be formulated without reference to an explicit Lagrangian [15]. It has been shown in numerous applications that this type of model provides an excellent description of nuclear matter and of bulk nuclear properties throughout the periodic table [14–22]. Thus we can calibrate our hadronic equation of state at zero temperature and normal nuclear densities, and then extrapolate into the regime of high density and temperature appropriate for the phase transition. The model we study involves cubic and quartic isoscalar self-couplings. Although nonlinear ρ meson interactions are possible [23], the nuclear symmetry energy is achieved using the simplest possible coupling of the ρ meson field to the nucleon. The pions are incorporated by adding their one-body contribution, *i.e.*, the contribution of an ideal Bose gas with an effective chemical potential,

to the thermodynamic potential. The effective chemical potential is chosen such that the ρ meson field couples to the total isospin density, which receives a contribution from nucleons and pions.

At low temperatures, the qualitative features studied here depend strongly on the nuclear symmetry energy. At higher temperatures, the inclusion of the pions is crucial due to the onset of a pion condensate in very asymmetric systems. The pions are incorporated in a very simple manner. Generally the isovector dependence of the hadronic EOS may be more complicated than in our model; however, these properties are not well known, particularly when one is far from symmetric matter. In this context it is important to realize that the hadronic model is formulated in terms of effective degrees of freedom. The two conserved charges, baryon number and total isospin, are the relevant quantities in the thermodynamic analysis whereas the particle numbers of the individual species may change when parameters, *e.g.*, temperature and pressure, vary. In the present case the pion condensed phase resembles closely matter containing Δ -resonances, which we could include in our model as well as other unstable nucleon resonances. However, we expect that this will not change the qualitative features of the EOS, since it depends only on the *total* baryon number and isospin.

Although our EOS can be calibrated very accurately at zero temperature and normal nuclear densities, the extrapolation into the regime of high densities is not unique. In the context of neutron star calculations it has recently been demonstrated [23] that the high density EOS is sensitive to combinations of parameters that are difficult to calibrate at normal densities. As a consequence, large uncertainties in the predictions arise. The density regime where the transition of hadronic matter to a quark–gluon plasma takes place corresponds to the interior region of a neutron star. Therefore similar difficulties can be expected. Although this limits the quantitative results of our analysis, the qualitative features of the basic physics remain unchanged.

Studies of the deconfinement phase transition in terms of a separate description of the two phases have a long history in the literature. In particular, in the context of neutron star matter, many calculations similar to ours have been performed earlier [8,10–13,24,25].

The first analysis which considered the transition in a system with two conserved charges was performed by Glendenning [8], with the restriction to zero temperature and to neutron star matter, *i.e.*, matter in beta-decay equilibrium. Along these lines the effect of neutrino trapping on the composition of cold protoneutron stars with quark cores has been investigated more recently [24]. We will extend the analysis to systems at arbitrary temperature, baryon density and isospin. By definition, the two-phase model cannot reveal the actual nature of the transition. In contrast, other phenomenological approaches which are directly inspired by the symmetries of QCD, for example linear sigma models [26], have been applied to shed more light on the fundamental properties of the transition. However, whether it is of first or second order or a cross-over phenomenon can only be established by full QCD studies, *i.e.*, by lattice calculations. We believe that, until this information is available, our approach is useful for providing a first orientation of the qualitative features which arise in the phase diagram of strongly interacting matter at finite baryon density and isospin. At zero baryon density the two-phase model implies a first-order transition. Starting from there our results are qualitatively similar to what was found in case of the liquid–gas phase transition of nuclear matter [9]. Primarily, the transition of hadrons to quarks and gluons in asymmetric systems is of *second order*, in contrast to the first-order transition that occurs in symmetric matter (which behaves like a one-component system). That means that some thermodynamic variables, *e.g.*, the entropy, are continuous and smooth throughout the transition, whereas the first-order transition is characterized by discontinuities in these quantities. Furthermore, we find that the transition regime in terms of densities and temperatures varies significantly with the isospin of the system. In particular the density at the onset of the transition is always lower in asymmetric matter. This result led us to the conclusion that it is more likely that the transition region is reached in collisions of very neutron-rich nuclei.

The outline of this paper is as follows: In Sec. II, we briefly summarize the general discussion of phase transitions in multicomponent systems which can be found in greater detail in Ref. [9]. We focus on the new aspects which arise when a thermodynamic sys-

tem is described by two different equations of state. In Sec. III, we describe the models for the two phases and summarize the relations that determine the equation of state. In Sec. IV, we apply our model to the deconfinement phase transition. We study the phase coexistence region and illustrate different thermodynamic processes by the aid of various phase diagrams and Maxwell constructions. We consider special situations which arise during ultra-relativistic heavy-ion collisions. We also discuss the parameter dependence of the thermodynamic features. Sec. V contains a short summary.

II. PHASE TRANSITIONS IN MULTICOMPONENT SYSTEMS

We consider a system characterized by a set of n mutually commuting charges Q_i . The thermodynamic features of such a system have been discussed earlier [7,9] in connection with the liquid-gas phase transition of asymmetric nuclear matter. Here we will focus on the situation where the system can exist in two phases each characterized by a *different* equation of state. The partition function might be generated by a Hamiltonian which is formulated in terms of different degrees of freedom in each phase [8]. For example, the elementary constituents (quarks and gluons) would be used in the first phase and composite particles (hadrons) in the second. As mentioned in the introduction, it is important to keep in mind that the conserved *charges* are the relevant quantities in the thermodynamic analysis. A conserved charge does not necessarily imply an independent particle species which may change during a process (by decay, for example); it includes any conserved quantity resulting from the underlying symmetries of the system, for example, isospin, baryon number, electric charge, *etc.*

To describe the equilibrium state of the system in phase α ($\alpha = 1, 2$) enclosed in a volume V we choose the Helmholtz free energy F

$$F_\alpha(T, V, Q_i) \equiv V\mathcal{F}_\alpha(T, \rho_i) \quad , \quad \alpha = 1, 2 \quad (1)$$

with

$$\rho_i = \frac{Q_i}{V} \quad , \quad i = 1, \dots, n .$$

Depending on the value of the free energy the system will be realized in one phase or the other or in a mixture of both, indicating a phase transition. To be more precise, the system in phase α will be stable against separation into two phases if the free energy of the single phase α is lower than the free energy in all two-phase configurations. This requirement can be formulated as

$$\mathcal{F}_\alpha(T, \rho_i) < (1 - \lambda)\mathcal{F}_\alpha(T, \rho_i^\alpha) + \lambda\mathcal{F}_\beta(T, \rho_i^\beta) \quad , \quad \alpha, \beta = 1, 2 \quad , \quad (2)$$

with

$$\rho_i = (1 - \lambda)\rho_i^\alpha + \lambda\rho_i^\beta \quad , \quad 0 < \lambda < 1 . \quad (3)$$

Note that this also implies

$$\mathcal{F}_\alpha(T, \rho_i) \leq \mathcal{F}_\beta(T, \rho_i) \quad , \quad (4)$$

so if Eq. (2) is satisfied, phase α is not only stable against phase separation, it is also the energetically favorable single-phase configuration. We assume that each single phase by itself describes a stable configuration¹, so that Eq. (2) is satisfied for $\alpha = \beta$, *i.e.*, the free energy in each phase is a convex function of the densities [27]. The last equation (3) ensures that the overall charges are conserved:

$$V\rho_i = V^\alpha\rho_i^\alpha + V^\beta\rho_i^\beta \quad \text{with} \quad V = V^\alpha + V^\beta . \quad (5)$$

Equation (2) is a *global* criterion for the stability of a one-phase configuration. Whenever it is violated, a system with two phases is energetically favorable. The phase coexistence

¹ When it actually happens that the free energy of one of the single phases describes an unstable configuration, *e.g.*, due to the liquid-gas phase transition in nuclear matter, we take \mathcal{F}_α to be the free energy resulting from a Maxwell construction in the unstable region, which is convex.

is governed by the Gibbs' conditions [29] demanding equal pressure p , temperature T and chemical potentials μ_i in both phases

$$\mu_i^\alpha(T, \rho_i^\alpha) = \mu_i^\beta(T, \rho_i^\beta) , \quad (6)$$

$$p^\alpha(T, \rho_i^\alpha) = p^\beta(T, \rho_i^\beta) . \quad (7)$$

It is important to realize, however, that under conditions of phase separation, Eq. (2) may still be valid *locally*, that means, in some small region $U = \{T, \rho_i\}$ of parameter space, but it may nevertheless be possible to find significantly different densities ρ_i^α and ρ_i^β in a larger domain $U \subset G$ that violate this condition. This leads to the existence of metastable states.

The two sets of densities $\{\rho_i^\alpha, \rho_i^\beta\}$ that satisfy Eqs. (6) and (7) form a surface in the parameter space $\{T, \rho_i\}$; this is the phase separation boundary, or binodal. For n conserved charges and two coexisting phases, Gibbs' phase rule implies that the binodal is an n -dimensional surface [29]. It can also be shown that this surface encloses all points that lead to a single (unstable) configuration with a higher value for the free energy [9].

The binodal surface determines the stability boundaries of the system. The mixed phase inside must be determined by a Maxwell construction. This is achieved by solving Eq. (3) [7,9] for given values of ρ_i , with ρ_i^α and ρ_i^β lying on the binodal surface. The free energy in the transition region is then given by

$$\mathcal{F}(T, \rho_i) = (1 - \lambda)\mathcal{F}_\alpha(T, \rho_i^\alpha) + \lambda\mathcal{F}_\beta(T, \rho_i^\beta) . \quad (8)$$

Densities related to other extensive quantities can be computed accordingly.

These ideas are illustrated in Fig. (1). We show the free energy density in both phases as a function of the density coordinates $\{\rho_i\}$ at constant temperature. At the location of the points B_1 and B_2 , the system enters the binodal region. In between, a phase mixture is energetically favorable. The free energy of the mixed phase as it results from the Maxwell construction Eq. (8) is indicated by the solid line which connects B_1 with B_2 . The dotted lines correspond to the free energy of the single-phase configurations. Between the point of intersection I and B_1 and between I and B_2 lie the metastable states of phase 1 and phase 2,

respectively. The configurations beyond I are unstable. Here not only a phase mixture but also the single (metastable) configuration of the opposite phase is energetically favorable. Instability normally arises due to fluctuations, which no longer can be restored by the system. This is signaled by the violation of a local stability criterion, *e.g.*, a negative compressibility. However, our description is based purely on the energetics and cannot provide information about the physical mechanism which leads to instability. This is certainly an indication that the separate description of the two phases breaks down at this point.

We close this section by specializing the general formalism to asymmetric matter. In the hadronic phase it consists of strongly interacting nucleons and mesons, and in the deconfined phase, weakly interacting quarks and gluons. For two quark flavors such a system is characterized by two conserved charges: the total baryon number

$$N_B \equiv V \rho_B \quad (9)$$

and the third component of isospin

$$I_3 \equiv \frac{1}{2} V \rho_3 . \quad (10)$$

Thus we have for the thermodynamic potential, or equivalently the pressure,

$$\frac{\Omega_\alpha}{V}(T, \mu_B^\alpha, \mu_3^\alpha) = -p^\alpha = \mathcal{F}_\alpha(T, \rho_B, \rho_3) - \mu_B^\alpha \rho_B - \frac{1}{2} \mu_3^\alpha \rho_3 , \quad (11)$$

where the baryon and isospin chemical potentials are given by

$$\mu_B^\alpha = \left(\frac{\partial \mathcal{F}_\alpha}{\partial \rho_B} \right)_{T, \rho_3} , \quad \mu_3^\alpha = 2 \left(\frac{\partial \mathcal{F}_\alpha}{\partial \rho_3} \right)_{T, \rho_B} . \quad (12)$$

In the discussion of asymmetric systems it is also useful to introduce the isospin ratio

$$x \equiv \frac{I_3}{N_B} = \frac{\rho_3}{2\rho_B} , \quad (13)$$

so that the free energy can be rewritten as

$$\mathcal{F}_\alpha(T, \rho_B, \rho_3) = \mathcal{F}_\alpha(T, \rho_B, x) . \quad (14)$$

III. THE EQUATION OF STATE

To generate the nuclear equation of state in the hadronic phase, we adopt the relativistic mean-field approach of Refs. [15,23] involving valence Dirac nucleons and effective mesonic degrees of freedom, which are taken to be neutral scalar (ϕ) and vector fields (V^μ), plus the isovector ρ meson (\mathbf{b}^μ) and pion field ($\boldsymbol{\pi}$). The basic quantity here is the thermodynamic potential as a functional of the meson mean fields which, in principle, can be formulated without reference to an explicit lagrangian. For homogeneous nuclear matter, at finite temperature and chemical potentials (μ_B, μ_3), it is of the general form [23]

$$\begin{aligned} \frac{\Omega}{V}(T, \mu_B, \mu_3; \phi, V_\nu, \mathbf{b}_\nu, \boldsymbol{\pi}) = & \frac{\Omega_N}{V} + \frac{\Omega_M}{V} + \frac{1}{2} m_s^2 \phi^2 - \frac{1}{2} m_v^2 V_\mu V^\mu - \frac{1}{2} m_\rho^2 \mathbf{b}_\mu \cdot \mathbf{b}^\mu + \frac{1}{2} m_\pi^2 \boldsymbol{\pi}^2 \\ & + \Delta\mathcal{V}(T, \mu_B, \mu_3; \phi, V_\mu, \mathbf{b}_\nu, \boldsymbol{\pi}) . \end{aligned} \quad (15)$$

The first two terms in Eq. (15), Ω_N/V and Ω_M/V , are the one-body contributions due to valence nucleons and mesons. The nonlinear potential $\Delta\mathcal{V}$ represents the unknown part of the thermodynamic potential, which includes the effects of nucleon exchange and correlations, as well as contributions from the quantum vacuum [15,32].

Following Ref. [9] the one-body fermionic contribution can be written as

$$\frac{\Omega_N}{V} = -\frac{1}{3\pi^2} [H_5(\nu_p, M^*) + H_5(\nu_n, M^*)] , \quad (16)$$

where the integral H_5 as well as others will be defined shortly. The corresponding contributions of the heavy meson fields ($\phi, V^\mu, \mathbf{b}^\mu$) to Ω_M are negligible in the relevant temperature range ($T \lesssim 200$ MeV). Thus we keep only the pions and write

$$\frac{\Omega_M}{V} = \frac{\Omega_\pi}{V} = -\frac{1}{6\pi^2} [B_5(\nu_\pi, m_\pi) + \frac{1}{2} B_5(0, m_\pi)] , \quad (17)$$

where the first term is the contribution of the charged pions [30,31], and the latter arises from the π^0 . The nonlinear potential $\Delta\mathcal{V}$ can be expanded in a Taylor series in terms of the meson mean fields [15,23]. In the normal phase of nuclear matter, *i.e.*, without a pion condensate, the pion mean field vanishes and the pions contribute only to the coefficients of

this series via loops. In practice, the series must be truncated, and the unknown coefficients serve as model parameters, which are chosen to reproduce certain empirical properties of equilibrium nuclear matter, as discussed below. For our calculation we choose the explicit form

$$\Delta\mathcal{V} = \frac{\kappa}{3!}\phi^3 + \frac{\lambda}{4!}\phi^4 - \frac{\zeta}{4!}g_v^4(V_\mu V^\mu)^2, \quad (18)$$

which includes a subset of the meson self-interactions up to fourth order in the fields. In principle, terms which couple different fields and also nonlinear interactions involving the ρ meson field are allowed [15]. We also disregard contributions involving the pion mean field which arise in the pion condensed phase. Although disregarding these couplings is “unnatural”, the present model defined by Eq. (18) is already general enough for our purposes. First of all, it can be accurately calibrated at normal densities, and it can be related to the most common models discussed in the literature. Unless one assumes scalar self-interactions only, the nonlinear couplings cannot be uniquely constrained by the calibration procedure, leading to uncertainties in the high-density EOS. In particular, little information is available to constrain contributions which explicitly depend on the pion field. Moreover, among these nonlinear terms, the quartic vector coupling in Eq. (18) is the most important one at high densities [23]. We will use this coupling to examine the uncertainties which arise in the quantitative predictions for the transition from hadrons to a quark-gluon plasma.

The mean fields are determined by extremization of the thermodynamic potential Eq. (15). The specific form of $\Delta\mathcal{V}$, introduced in Eq. (18), together with Eqs. (16) and (17), leads to the self-consistency equations

$$\frac{m_s^2}{g_s^2}\Phi + \frac{\kappa}{2g_s^3}\Phi^2 + \frac{\lambda}{6g_s^4}\Phi^3 = \rho_s, \quad (19)$$

$$W \left(1 + \frac{g_v^2}{m_v^2} \frac{\zeta}{6} W^2 \right) = \frac{g_v^2}{m_v^2} \rho, \quad (20)$$

$$R = \frac{g_\rho^2}{2m_\rho^2} \rho_3, \quad (21)$$

where the scalar and baryon densities are given by

$$\rho_s = \frac{M^*}{\pi^2} \left[H_3(\nu_p, M^*) + H_3(\nu_n, M^*) \right] , \quad (22)$$

$$\rho_B = \frac{1}{\pi^2} \left[G_3(\nu_p, M^*) + G_3(\nu_n, M^*) \right] . \quad (23)$$

The isospin density receives contributions from nucleons and pions

$$\begin{aligned} \frac{1}{2}\rho_3 &= \frac{1}{2}\rho_3^N + \frac{1}{2}\rho_3^\pi \\ &\equiv \frac{1}{2\pi^2} \left[G_3(\nu_p, M^*) - G_3(\nu_n, M^*) \right] + \frac{1}{2\pi^2} A_3(\nu_\pi, m_\pi) . \end{aligned} \quad (24)$$

The scaled meson fields are $\Phi \equiv g_s \phi$, $W \equiv g_v V_0$, and $R \equiv g_\rho b_0$, with b_0 the timelike, neutral part of the ρ meson field.

The baryon effective mass and effective chemical potentials are defined in terms of the meson mean fields and the baryon and isospin chemical potential as

$$M^* \equiv M - \Phi , \quad (25)$$

$$\nu_p \equiv \mu_B + \frac{\mu_3}{2} - W - \frac{1}{2} R , \quad (26)$$

$$\nu_n \equiv \mu_B - \frac{\mu_3}{2} - W + \frac{1}{2} R . \quad (27)$$

The effective chemical potential for the pions is given by

$$\nu_\pi \equiv \nu_p - \nu_n = \mu_3 - R , \quad (28)$$

so that the ρ meson field in Eq. (21) couples to the total isospin density in Eq. (24). We also introduce the required integrals over the thermal distribution functions as

$$G_n(\mu, M) \equiv \int_0^\infty k^{n-1} dk \left(\frac{1}{1 + e^{\beta[E(k, M) - \mu]}} - \frac{1}{1 + e^{\beta[E(k, M) + \mu]}} \right) , \quad (29)$$

$$H_n(\mu, M) \equiv \int_0^\infty \frac{k^{n-1} dk}{E(k, M)} \left(\frac{1}{1 + e^{\beta[E(k, M) - \mu]}} + \frac{1}{1 + e^{\beta[E(k, M) + \mu]}} \right) , \quad (30)$$

for fermions and

$$A_n(\mu, m) \equiv \int_0^\infty k^{n-1} dk \left(\frac{1}{e^{\beta[E(k, m) - \mu]} - 1} - \frac{1}{e^{\beta[E(k, m) + \mu]} - 1} \right) , \quad (31)$$

$$B_n(\mu, m) \equiv \int_0^\infty \frac{k^{n-1} dk}{E(k, m)} \left(\frac{1}{e^{\beta[E(k, m) - \mu]} - 1} + \frac{1}{e^{\beta[E(k, m) + \mu]} - 1} \right) , \quad (32)$$

for bosons, where $E(k, M) \equiv (k^2 + M^2)^{1/2}$, and $n > 0$ to ensure convergence is understood. Moreover, the boson integrals are subject to the constraint $|\mu| \leq m$.

By inserting the solution of Eqs. (19)–(21) into Eq. (15), it is straightforward to compute the pressure

$$p = -\frac{\Omega}{V} = -\frac{\Omega_N}{V}(T, \nu_p, \nu_n, M^*) - \frac{\Omega_\pi}{V}(T, \nu_\pi) + \frac{m_v^2}{2g_v^2} W^2 + \frac{\zeta}{24} W^4 + \frac{m_\rho^2}{2g_\rho^2} R^2 - \frac{m_s^2}{2g_s^2} \Phi^2 - \frac{\kappa}{6g_s^3} \Phi^3 - \frac{\lambda}{24g_s^4} \Phi^4. \quad (33)$$

Other quantities like the free energy, the entropy, *etc.*, follow by using standard thermodynamic relations.

For the quark-gluon phase we adopt a bag-model type EOS [12] involving massless u and d quarks ($N_f = 2$)

$$\frac{\Omega}{V}(T, \mu_B, \mu_3) = \frac{\Omega_{\text{pert}}}{V}(T, \mu_B, \mu_3) + b, \quad (34)$$

where Ω_{pert}/V is the perturbative expansion of the thermodynamic potential

$$\begin{aligned} \frac{\Omega_{\text{pert}}}{V}(T, \mu_B, \mu_3) = & -\frac{\pi^2}{45} T^4 \left(8 + \frac{21}{4} N_f \right) - \frac{1}{2} \sum_{f=u,d} \left(T^2 \mu_f^2 + \frac{\mu_f^4}{2\pi^2} \right) \\ & + \frac{2\pi}{9} \alpha_s \left(T^4 \left[3 + \frac{5}{4} N_f \right] + \frac{9}{2} \sum_{f=u,d} \left[\frac{T^2 \mu_f^2}{\pi^2} + \frac{\mu_f^4}{2\pi^4} \right] \right), \end{aligned} \quad (35)$$

and b is the difference between the energy density of the perturbative and the nonperturbative QCD vacuum, *i.e.*, the bag constant. The chemical potentials of the two flavors are connected to the baryon and isospin chemical potentials by

$$\mu_u = \frac{1}{3} \mu_B + \frac{1}{2} \mu_3, \quad \mu_d = \frac{1}{3} \mu_B - \frac{1}{2} \mu_3, \quad (36)$$

which allows the computation of the corresponding densities according to

$$\rho_B = - \left(\frac{\partial \Omega}{\partial \mu_B} \frac{1}{V} \right)_{T, \mu_3}, \quad \frac{1}{2} \rho_3 = - \left(\frac{\partial \Omega}{\partial \mu_3} \frac{1}{V} \right)_{T, \mu_B}. \quad (37)$$

We close this section with a short description of the calibration of the EOS. The model for the hadronic phase has six free parameters. Following Ref. [15] we choose the value of

the coupling ζ and determine the other parameters so that the five equilibrium properties of nuclear matter, as listed in Table I, are reproduced. The free parameter ζ is chosen within the natural range $0 \leq \zeta \leq 0.06$ [15,23]. To fix the two parameters in the quark-gluon phase, namely the bag constant b and the strong coupling constant α_s , we proceed as follows. We specify the bag constant to $b = 160 \text{ MeV}/\text{fm}^3$ and determine α_s so that our model reproduces a transition temperature of 150 MeV at zero baryon density, which is in the currently accepted temperature range [34]. As a consequence of this calibration α_s depends on ζ . This dependence, however, is extremely weak. The value $\alpha_s = 0.349$ obtained for $\zeta = 0$ changes only by 0.1% when ζ is varied within the natural range.

IV. PHASE STRUCTURE OF ASYMMETRIC MATTER

In this section we apply the formalism of Sec. II to the deconfinement phase transition. Within our simple two-phase model we consider highly excited asymmetric matter created in an ultra-relativistic collision of two heavy-ions. The dynamical evolution of the system during the collision is a very complex process and it is convenient to divide the reaction into three stages: the formation of a highly excited matter system, its expansion and the eventual decay. The question of whether the required energy densities can be achieved in an experiment to form a quark-gluon plasma during the first violent stage is a difficult one, which we will not attempt to answer here. We simply assume that such a state arises and ultimately reaches equilibrium at some finite temperature, density and pressure. We follow the subsequent expansion of the system during the second stage and concentrate on the new features of the phase diagram that arise as a function of the total isospin. Although our general discussion will encompass the entire range of $x \leq 0$, we will study systems with $-0.2 \leq x \leq 0$ and $x = -0.5$ in more detail to obtain estimates for the size of the new effects. The former range covers the isospin ratios which are experimentally accessible in heavy-ion collisions, e.g., $x_{\text{Au+Au}}, x_{\text{U+U}} \approx -0.1$, whereas the latter value corresponds to neutron matter relevant in astrophysical applications.

As discussed in the context of the liquid-gas phase transition of asymmetric nuclear matter [7,9], the phase structure of binary systems is more complex than in one-component systems. The basic quantity in the analysis is the phase separation boundary or binodal, which forms a two-dimensional surface in parameter space as discussed in Sec. II. Before we discuss the binodal structure of the deconfinement phase transition as it arises in our model, let us briefly point out the role of the pions. To this end, assume our system is prepared in the hadron phase at some fixed isospin ratio x , as defined in Eq. (13), and let us follow an isothermal compression. At some critical baryon density ρ_B^c the chemical potential of the pions will approach the (negative) value of the pion mass, *i.e.*,

$$\nu_\pi \rightarrow -m_\pi \quad \text{for} \quad \rho_B \rightarrow \rho_B^c, \quad (38)$$

indicating the onset of a pion condensate [29]. The critical density depends on x and on T , and will be smaller in more asymmetric systems. At this point a macroscopically occupied π^- mode arises which is characterized by a nonvanishing pion mean field. In principle, the corresponding contributions to the thermodynamic potential in Eq. (15) must now be kept explicitly, and the value of the mean field is determined by minimization [30,35]. As discussed in the last section we will disregard the explicit mean-field contributions of the pions in the following. That means we neglect the pion-nucleon as well as the pion self-interactions. To incorporate the condensed phase consistently we will be satisfied to add the contribution of the zero-momentum states of the pions to the isospin density in Eq. (24)

$$\frac{1}{2}\rho_3^\pi = -2m_\pi\kappa^2 + \frac{1}{2\pi^2}A_3(-m_\pi, m_\pi), \quad (39)$$

where the effective chemical potential

$$\nu_\pi = \nu_p - \nu_n = -m_\pi \quad (40)$$

is held fixed in the condensed phase. The parameter κ^2 is the continuous order parameter of this transition, which specifies the amount of isospin charge carried by the zero-momentum states [30,31]. In contrast, the condensate does not contribute to the pressure of the system;

thus, one simply substitutes the value of ν_π , as given by Eq. (40), in the expression for the hadronic pressure Eq.(33). We will leave the study of the contributions arising from pionic interactions as an important topic for future work.

We now return to the general discussion of the phase diagram in our system. We begin the analysis with $\zeta = 0$ for the value of the quartic vector meson coupling in the hadronic EOS. We will study the influence of this parameter at the end of this section.

The binodal is determined by Gibbs' conditions (6) and (7) which enforce equal pressure and chemical potentials for the hadronic phase and for the quark–gluon phase in equilibrium. In general these two phases have a different isospin ratio x . The binodal surface in $\{x, p, T\}$ space is indicated in Fig. 2. A sequence of several slices at fixed T is shown. For a given temperature, the binodal section is divided into two branches. One branch, at the lower pressure, describes the system in the hadron phase, while the other branch, at the higher pressure, describes the quark–gluon phase. These two branches contain the beginning and ending configurations of the phase transition. The shape of the binodal slices changes drastically between $T = 0$ and $T = 150$ MeV. One observes that the enclosed area becomes smaller with increasing temperature until, at $T_c = 150$ MeV, the two branches coalesce to a single line at constant pressure $p = 19.08$ MeV/fm³ with isospin ratios ranging from $x \approx -4.5$ to $x = 0$. This line of critical points marks the transition point of systems at zero baryon density.

Another important observation is that the pressure steadily decreases when the temperature increases. At the same time, the transition regime, *i.e.*, the difference in pressure between the two phases at the beginning and at the end of a transition, becomes smaller. Also indicated in Fig. (2) are the special configurations that separate into two phases with the same isospin ratio. The coordinates of these configurations form the two lines of equal concentration (LEC), one of which coincides with the projection $x = 0$ in our system. The isospin ratio of the second LEC increases with temperature and eventually the two LEC intersect at $T \approx 137.2$ MeV. For a fixed temperature the pressure necessarily attains an extremum at the points of equal concentration [29].

Generally, the hadronic configurations are divided into normal states and states exhibiting a pion condensate. The coordinates of the configurations at the onset of the condensation also form a two-dimensional surface. This critical surface can be parametrized in terms of two coordinates in $\{x, p, T\}$ space, *e.g.*, as $p_c(x, T)$. The intersection of the critical surface with the binodal forms the line of three phases (LTP), which marks the onset of the pion condensate on the hadronic branch². In Fig. (2) these states are emphasized by the bold dashed lines. The isospin ratio of the LTP decreases with increasing temperature. Above $T \approx 136.2$ MeV the critical pressure curve and the binodal no longer intersect.

The binodal in $\{\rho_B, x, T\}$ space is indicated in Fig. (3), where several branches at different x are projected onto the $\{\rho_B, T\}$ plane. The onset of the condensate, *i.e.*, the critical temperature as a function of the baryon density and isospin ratio, is marked by an open circle. Note the change of density in the two-phase region. The most extreme situations are encountered at $T = 0$. For example, in symmetric matter the density increases between the onset and the completion of the transition by more than $3.5\rho_B^0$. This density regime becomes even larger in asymmetric systems. Another important observation is that the density at the onset decreases with increasing asymmetry. If we compare these points for $x = 0$ and $x = -0.2$ at $T = 0$ we find an decrease of $\Delta\rho_B \approx 0.5\rho_B^0$.

The role of the pions becomes more apparent in Fig. (4). Part (a) indicates one slice of Fig. (2) at $T = 50$ MeV. Also included is the projection of the critical surface in the form of the critical pressure curve $p_c(x)$. Nuclear matter in the normal phase resides on the right-hand side, and the states with a pion condensate on the left-hand side. The critical curve intersects the binodal at TP. In contrast, the pion contributions are not included in part (b). With nucleons only, the isospin ratio in the hadronic branch is limited by

²Since there is no two-phase coexistence in a Bose condensation, the LTP is not a line of triple points which could arise in a binary system [29]. The LTP is merely a boundary between areas in parameter space which describe two different two-phase configurations.

$-0.5 \leq x \leq 0$ which leads to a widely open binodal surface. Furthermore, only one point of equal concentration arises (at $x = 0$).

To illustrate the phase-separation scenarios, we study the behavior of matter under an isothermal compression. Assume that the system is initially prepared in the hadronic phase with isospin ratio $x = -0.4$ and $p \lesssim 50 \text{ MeV/fm}^3$. The situation is also indicated in part (a) of Fig. 4. During the compression, the system first crosses the critical pressure curve at the point A , where pion condensation begins. Starting with $\kappa^2 = 0$ at A the contribution of the condensate to the (fixed) isospin ratio increases during the compression. At the point B the two-phase region is encountered and now a quark–gluon phase is about to emerge. The solution of Gibbs’ conditions (6) and (7) determine the density and the isospin ratio x_C of this new phase, which occurs at the point labeled C . As the system is compressed, the *total* isospin ratio x remains fixed, as dictated by the conservation laws, but the hadronic phase evolves from B to E , while the quark–gluon phase evolves from C to D . At the point D , the system leaves the region of instability. The original hadronic phase (which now has no pion condensate) is about to disappear, and it exists in an infinitesimal volume with a density and isospin ratio x_E corresponding to the point E .

An important observation is that if the system encounters the binodal between the two points of equal concentration then the quark–gluon phase is always more asymmetric and has a higher baryon density than the hadronic phase. This behavior is due to the *symmetry energy*, which is higher in the hadronic phase. Therefore it is energetically favorable for asymmetric matter to separate into a denser and more asymmetric quark–gluon phase and a hadronic phase that is more dilute and symmetric.

The energetics also implies a significant simplification if the system is initially prepared with an isospin ratio corresponding to one of the points EC. It is now energetically favorable for the system to separate into two phases with the same composition. In this so-called “indifferent equilibrium” [36], matter behaves like a one–component system (see also the discussion in [9]). In contrast to the previous case the system becomes unstable at one of the points EC in Fig. 4 and stays at this point until the transition is completed. Note that

the location of the point EC at $x = 0$ is model independent since symmetric matter is always the configuration with lowest energy. The location of the second point depends on specific model features, particularly on the predicted values for the symmetry energy and on the pionic contributions.

The results of the corresponding Maxwell constructions are indicated in Fig. 5. We consider different isospin ratios at $T = 0$ in part (a) and at $T = 50$ MeV in part (b), respectively. For symmetric matter ($x = 0$), we obtain the familiar result with a constant vapor pressure, represented by a horizontal line. At $x < 0$ the equal demand of Gibbs' conditions and the conservation of the overall isospin forces the pressure to change during the transition. Also shown in Fig. 5 are isotherms for "neutron matter" ($x = -0.5$). The name is somewhat misleading since the system contains a finite number of protons even without the pions. It is common in the literature [23,10,11,25] to treat neutron matter as a single-component system. The qualitatively different features which arise in a proper treatment as a system with *two* conserved charges have been pointed out earlier by Glendenning [8] in the context of neutron star calculations (see also Ref. [24]). In addition, part (b) of Fig. 5 also includes a system with an isospin ratio which corresponds to the second point of equal concentration. As discussed above, this system also stays at a constant vapor pressure throughout the transition.

The change of the pressure throughout the phase separation in asymmetric systems is an indication of a *smoother* transition than in symmetric or one-component systems. A more precise characterization of the transition can be obtained from the isobaric process indicated in Fig. (6). The entropy as a function of temperature for three different isospin ratios is shown. In symmetric matter we find a discontinuity at the transition temperature, which gives rise to a latent heat Q_L , *i.e.*, all the heat is used to convert hadrons into quarks. In asymmetric matter the entropy remains smooth but the temperature now changes throughout the transition so that no strict latent heat can be assigned to this process. For example, the isospin ratio $x = -0.2$ shown in Fig. (6) gives rise to a temperature change of $\Delta T \approx 30$ MeV. As discussed in more detail in Ref. [9], these are the features which

lead to a first-order transition in symmetric matter and to a second-order transition in the asymmetric system, according to Ehrenfest’s definition.

The processes we have considered so far correspond to very specific idealized situations and served mainly to study the basic thermodynamic features of our system. Generally, it is not clear if the expansion of the highly excited matter created in a heavy-ion collision can be described by a distinct thermodynamic process. However, the situation simplifies at extremely high collision energies. In this so-called scaling regime, the colliding nuclei become transparent and the excited plasma is created between the two nuclei when they recede from the collision point. The basic assumption here is that the total entropy is created in the initial stage of the collision and remains nearly constant during the later evolution. Under this assumption, the expansion of the plasma is nearly adiabatic and can be described by relativistic hydrodynamics [37,38].

To make contact with this discussion, we also studied adiabatic processes. The properties of the system in the (ρ_B, T) plane can be studied in Fig. (7). Adiabats for various values of the entropy per baryon are indicated for symmetric matter in part (a) and for asymmetric matter in part (b), respectively. The dashed lines are the coexistence curves, *i.e.*, the projection of the hadronic and the quark-gluon branch of the binodal, which intersect at the critical point CP. The curves in the coexistence region are the result of a Maxwell construction. Note the behavior of the system in the mixed phase. Throughout the transition the temperature *decreases* with increasing density, in contrast to the pure phases where the temperature increases monotonically. This peculiar behavior arises because for a given baryon density and temperature, the entropy in the quark-gluon phase is always higher. If we think in terms of a “boiling” or “condensation” process and compare to a liquid-gas transition one would expect the opposite behavior ³. In an ordinary liquid the high-density

³A system which exhibits a similar behavior is the liquid-solid phase transition of ³He, for which the entropy in the high-density solid phase is higher than in the low-density liquid phase due to

phase has the lower entropy and the temperature would rise steadily during the transition.

If we compare the extension of the transition regime in the symmetric and asymmetric systems, we find a similar quantitative difference as observed in the previous discussion. Generally, for a given value of the entropy per baryon, the onset of the transition occurs at a lower density and temperature in asymmetric matter. For example, if we compare the adiabat $S/N_B = 2$ in Fig. (7a) and (7b), the density decreases by $\Delta\rho_B \approx \rho_B^0/3$ and the temperature by $\Delta T \approx 4$ MeV. Compared to the overall scale set by the critical temperature of 150 MeV this temperature difference is certainly less significant. However, the qualitative difference between the two systems could be an indication that the transition region is experimentally better accessible in a collision of extremely neutron-rich systems, which might be obtainable with radioactive beams.

Finally, we briefly discuss how the properties of the phase transition change when the parameter ζ in the hadronic EOS is varied. This point has been discussed in Ref. [23] for pure neutron matter and here we will extend the analysis to arbitrary isospin ratios. Up to now the hadronic EOS in Eq. (33) was generated without the quartic vector meson interaction. In the following we allow a nonzero coupling within the natural range $0 \leq \zeta \leq 0.06$.

Figure (8) shows the baryon density at the onset and at the end of the transition for the isospin ratios $x = 0, -0.2, -0.5$ at $T = 0$. Note that all values of ζ reproduce identical properties of nuclear matter and a transition temperature of $T = 150$ MeV at zero baryon density. Generally, one observes that for arbitrary isospin ratios, increasing ζ softens the EOS, which leads to substantially higher transition densities. The increase in the symmetric system is remarkable (note the logarithmic scale); at sufficiently large values of ζ the transition vanishes altogether. The transition is driven by the energetics in both phases and therefore this behavior is most easily understood by examining the high-density limit of the energy per baryon [23]. Using Eq. (35) and the relation $\mathcal{E} = 3p + 4b/3$, one obtains for the

the spin disorder present in the solid phase [39].

quark phase

$$\lim_{\rho_B \rightarrow \infty} \mathcal{E}_Q / \rho_B = c_Q \rho_B^{1/3} . \quad (41)$$

The asymptotic behavior of the hadronic EOS depends on ζ and x . For $x < 0$, $\zeta \geq 0$ or $x = 0$, $\zeta = 0$ the quadratic terms in Eq. (33) dominate, which leads to

$$\lim_{\rho_B \rightarrow \infty} \mathcal{E}_H / \rho_B \propto \rho_B . \quad (42)$$

Thus, at sufficiently high densities, the hadronic matter always has higher energy compared to the quark phase and a transition is possible.

A special situation arises for $x = 0$ and $\zeta > 0$. In this case the leading behavior is, up to the prefactor, identical to Eq. (41), *i.e.*,

$$\lim_{\rho_B \rightarrow \infty} \mathcal{E}_H / \rho_B = c_H \rho_B^{1/3} . \quad (43)$$

By comparing the factors c_Q and c_H in Eq. (41) and in Eq. (43), respectively, one arrives at the remarkable result that a transition is possible only if (see also the discussion in [23])

$$\frac{1}{3} \left[1 + \left(\frac{4}{\pi^2 \zeta} \right)^{1/3} \right] > 1 + \frac{2\alpha_s}{3\pi} . \quad (44)$$

This implies that for sufficiently large values of the nonlinear coupling, *symmetric matter remains in the hadron phase*. Note that we would arrive at this result for *arbitrary* isospin ratios if we included an additional quartic ρ meson coupling. In accordance with Ref. [23], we conclude that the parameter dependence of the hadronic EOS at high densities leads to large uncertainties in the predictions for the transition region of the deconfinement phase transition (if it exists). In principle, reproducing the quantitative features of the transition could be a tool for calibrating the hadronic EOS better in the high-density region. However, more information is required than available at present, and quantitative predictions are limited.

V. SUMMARY

In this paper we studied the deconfinement phase transition from hadronic matter to a quark-gluon plasma as a function of the isospin. The analysis was based on a separate description of the hadronic and the quark-gluon phase. We have demonstrated that in a consistent treatment of the two conserved charges, baryon number and isospin, qualitatively new features arise. Most importantly, the phase transition in asymmetric matter is generally continuous and of second-order. This is in contrast to the discontinuous first-order behavior of symmetric systems, which arise as singular points in the phase diagram of asymmetric matter.

The analysis was based on the determination of the phase separation boundary, the binodal, which indicates the region where a separation into two phases is energetically favorable. The binodal is determined by Gibbs' criteria for phase equilibrium. In a system with two conserved charges, it forms a two-dimensional surface in parameter space, in contrast to the one-dimensional surface in one-component systems. The greater dimensionality leads to the qualitatively new behavior. Primarily, the transition in asymmetric matter is continuous and of second order. We saw that the pressure, temperature and isospin ratios in the participating phases change throughout the transition. That means that in general, asymmetric systems pass through a transition region rather than staying at a transition point which leads to discontinuities in one-component and symmetric systems.

To apply these results to the deconfinement phase transition in nuclear matter, we employed a simple two-phase model. The hadronic EOS was generated in a relativistic mean-field model involving the interaction of baryons with isoscalar scalar and vector fields and with the isovector ρ meson and pion field. This model involves cubic and quartic isoscalar self-couplings and allows for an accurate calibration at normal nuclear densities to reproduce bulk properties of finite nuclei and nuclear matter. For the description of the quark-gluon phase, we adopted a bag-model type EOS involving massless u and d quarks. In this framework thermodynamic quantities consists of two parts. A perturbative contribution, where

we included the first order correction in the strong coupling constant, and a nonperturbative contribution, represented by the bag constant, which accounts for the QCD trace anomaly. Guided by recent results from lattice calculations, we chose the bag constant and the strong coupling constant to reproduce a transition temperature of 150 MeV for matter at zero baryon density. However, the calibration of the hadronic EOS at normal densities is not unique and predictions at high densities are sensitive to the model parameters. By studying variations of the quartic vector meson coupling within the natural range, we found significant uncertainties in the predictions for the onset of the deconfinement phase transitions in systems at finite baryon density. For sufficiently large values of this coupling the hadronic EOS becomes so soft that the transition vanishes altogether.

This two-phase model was then used to study the deconfinement phase transition in highly excited matter that is produced in ultra-relativistic heavy-ion collisions. By construction, an approach based on a separate description of the two phases cannot reveal the actual nature of the transition. However, until more concrete and reliable lattice calculations are available, we believe that despite this limitation our analysis is useful for providing a first orientation and concrete description of the qualitative features which arise in the phase diagram of strongly interacting *asymmetric* matter. There are several significant differences between the phase diagram for an asymmetric system and that for symmetric matter. In the first place, the location of the transition region in parameter space depends on the isospin ratio of the system. Generally, the onset of phase separation occurs at lower baryon densities and temperatures in more asymmetric systems. More importantly, the dimensionality of the phase-separation region is larger in asymmetric matter leading to a *continuous* transition. This implies that the thermodynamic properties of the participating phases change throughout the transition. Although these effects are small for realistic isospin ratios $x \approx -0.1$, the trend in the isospin dependence to lower densities and temperatures could be an indication that the transition region is easier to reach in collisions of very neutron rich nuclei, which might be created in radioactive beam facilities.

The analysis also revealed interesting physics in the isovector channel. Most importantly,

the incorporation of the pions into the model for the hadronic phase was crucial for the shape of the binodal surface and therefore also for the path of the system through the mixed-phase region. The salient feature is the onset of a pion condensate at large baryon densities and in very asymmetric systems. This phenomenon is certainly of minor practical importance since the relevant isospin ratios lie beyond the experimentally accessible region. However, interest in Bose condensation has recently been revived in the literature, particularly since the possibility of kaon condensation in neutron star matter has been proposed [40]. Analyzing these effects in connection with the deconfinement phase transition provides an important topic for future work on this problem.

ACKNOWLEDGMENTS

I am pleased to thank B. D. Serot for many useful comments and stimulating discussions. This work was supported by the U.S. Department of Energy under contract No. DE-FG02-87ER40365.

TABLES

TABLE I. Equilibrium Properties of Nuclear Matter

k_F^0	ρ_B^0	M_0^*/M	e_0	K_0	a_4
1.30 fm^{-1}	0.1484 fm^{-3}	0.60	-15.75 MeV	250 MeV	35 MeV

REFERENCES

- [1] J. Stachel and G. R. Young, *Ann. Rev. Nucl. Part. Sci.* **42**, (1992) 537.
- [2] J. W. Harris and B. Müller, The search for the Quark-Gluon Plasma, to appear in *Ann. Rev. Nucl. Sci.* **46** (1996) 71.
- [3] G. Boyd, J. Engels, F. Karsch, E. Laerman, C. Legeland, M. Lutgemeier and B. Petersson, *Phys. Rev. Lett.* **75** (1995) 4169.
- [4] K. Kanaya, *Nucl. Phys. B (Proc. Suppl.)* **47**, (1996) 144.
- [5] F. R. Brown, F. P. Butler, H. Chen, N. H. Christ, Z. Dong, W. Schaffer, L. I. Unger, and A. Vaccarino, *Phys. Rev. Lett.* **65** (1990) 2491.
- [6] Y. Iwasaki, K. Kanaya, S. Kaya, S. Sakai and T. Yoshié, *Nucl. Phys. B (Proc. Suppl.)* **42**, (1995) 499.
- [7] M. Barranco and J. R. Buchler, *Phys. Rev. C* **22**, 1729 (1980).
- [8] N. K. Glendenning, *Phys. Rev. D* **46**, 1274 (1992).
- [9] H. Müller, and B. D. Serot, *Phys. Rev. C* **52**, 2072 (1995).
- [10] J. C. Collins and M. J. Perry, *Phys. Rev. Lett.* **34** (1975) 1353.
- [11] G. Baym and S. A. Chin, *Phys. Lett.* **62 B** (1976) 241.
- [12] J. Kuti, B. Lukács, J. Poonyi and K. Szlachányi, *Phys. Lett.* **95B** (1980) 75.
- [13] B. D. Serot and J. D. Walecka, *Adv. Nucl. Phys.* **16**, 1 (1986).
- [14] B. D. Serot, *Rep. Prog. Phys.* **55**, 1855 (1992).
- [15] R. J. Furnstahl, B. D. Serot, and H.-B. Tang, *Nucl. Phys. A* **598** (1996) 539.
- [16] J. Boguta and A. R. Bodmer, *Nucl. Phys. A* **292**, 413 (1977).
- [17] P. G. Reinhard, M. Rufa, J. Maruhn, W. Greiner, and J. Friedrich, *Z. Phys. A* **323**, 13

- (1986).
- [18] R. J. Furnstahl, C. E. Price, and G. E. Walker, *Phys. Rev. C* **36**, 2590 (1987).
- [19] R. J. Furnstahl and C. E. Price, *Phys. Rev. C* **40**, 1398 (1989).
- [20] A. R. Bodmer and C. E. Price, *Nucl. Phys.* **A505**, 123 (1989).
- [21] Y. K. Gambhir, P. Ring, and A. Thimet, *Ann. Phys. (N.Y.)* **198**, 132 (1990).
- [22] R. J. Furnstahl and B. D. Serot, *Phys. Rev. C* **47**, 2338 (1993).
- [23] H. Müller, and B. D. Serot, *Nucl. Phys.* **A606**, 508 (1996).
- [24] M. Prakash, J.R. Cooke and J.M. Lattimer, *Phys. Rev. D* **52**, 661 (1995).
- [25] B. D. Serot and H. Uechi, *Ann. Phys. (N.Y.)* 179 (1987) 272.
- [26] R. D. Pisarski and F. Wilczek, *Phys. Rev. D* **29**, 338 (1984).
- [27] A. W. Roberts and D. E. Varberg, *Convex Functions* (Academic Press, New York, 1973).
- [28] A. L. Fetter and J. D. Walecka, *Quantum Theory of Many-Particle Systems* (McGraw-Hill, New York, 1971),
- [29] L. D. Landau and E. M. Lifshitz, *Statistical Physics* (Pergamon Press, Oxford, 1969).
- [30] H. E. Haber and H. A. Weldon, *Phys. Rev. D* **25** (1982) 502.
- [31] J. I. Kapusta, *Finite-temperature field theory* (Cambridge University Press, Cambridge, 1989).
- [32] R. J. Furnstahl, H.-B. Tang, and B. D. Serot, *Phys. Rev. C* **52** (1995) 1368.
- [33] O. K. Kalashnikov and V. V. Klimov, *Phys. Lett.* **88B** (1979) 328;
J. I. Kapusta, *Nucl. Phys.* **B148** (1979) 461.
- [34] T. Blum, L. Kärkkäinen, D. Toussaint and S. Gottlieb, *Phys. Rev. D* **51** (1995) 5153.

- [35] G. Baym, Phys. Rev. Lett. **30** (1973) 1340.
- [36] R. Haase and H. Schönert, Int'l. Encyclopedia of Physical Chemistry and Chemical Physics, topic 13: *Mixtures, Solutions, Chemical, and Phase Equilibria*, vol. 1: *Solid-Liquid Equilibria* (Pergamon Press, NY, 1969).
- [37] C. B. Chiu, E. C. G. Sudarshan and K. H. Wang, Phys. Rev. D **12** (1975) 902.
- [38] J. D. Bjorken, Phys. Rev. D **27** (1983) 140.
- [39] N. Goldenfeld, *Lectures on phase transitions and the renormalization group* (Addison-Wesley, 1992).
- [40] H. D. Politzer and M. B. Wise, Phys. Lett. B 273 (1991) 156.

FIGURE CAPTIONS

FIG. 1. The Maxwell construction for a system with more than one conserved charge. The free energy density as a function of the densities $\{\rho_i\}$ at constant temperature is shown. The Maxwell construction is indicated by the segment $\overline{B_1B_2}$. The course of the free energy in each single phase is denoted by the dotted lines. The metastable configurations are located on $\overline{B_1I}$ and $\overline{B_2I}$ between the binodal and the point where the free energy curves intersect.

FIG. 2. The binodal surface indicating the two-dimensional phase-coexistence boundary in (p, T, x) space. A sequence of binodal sections at fixed temperature is shown. The points of equal concentrations (EC) and the points of three phases (TP) are indicated.

FIG. 3. Binodal section in (ρ_B, T, x) space. The projection of several binodal branches at different x onto the (ρ_B, T) plane is shown. The isospin ratios are $x = 0, -0.1, -0.2, -0.3, -0.4, -0.5$, starting from the right. The open circles mark the critical temperature for the onset of the pion condensate.

FIG. 4. (a) Binodal section at $T = 50$ MeV including the contributions of the pions in the hadronic phase. The points B through E denote phases participating in a phase transition. At A the system crosses the critical pressure curve which marks the onset of pion condensation. The point of three phases (TP) and the points of equal concentration (EC) are also indicated. (b) Binodal section at $T = 50$ MeV without the pionic contributions.

FIG. 5. (a) Isotherms for different values of x at $T = 0$. The isospin ratios are $x = 0, -0.1, -0.2, -0.3, -0.4, -0.5$ from the top to the bottom. (b) Isotherms for different values of x at $T = 50$ MeV. The isospin ratios are the same as in part (a). In addition the isotherm with $x_{EC} = -1.44$, which corresponds to the second point of equal concentration, is also indicated.

FIG. 6. Entropy per baryon as a function of temperature at constant pressure for various isospin ratios.

FIG. 7. Properties of nuclear matter as functions of temperature and density. The dashed lines denote the coexistence curves (CE), which intersect at the critical point (CP). The solid lines indicate adiabats. The lines between the coexistence curves are the stable mixed-phase configurations. Part (a) shows results for symmetric matter ($x = 0$) and part (b), for asymmetric matter with $x = -0.2$.

FIG. 8. Baryon density at the onset and at the end of the transition as a function of the quartic vector meson coupling ζ .

FIGURES

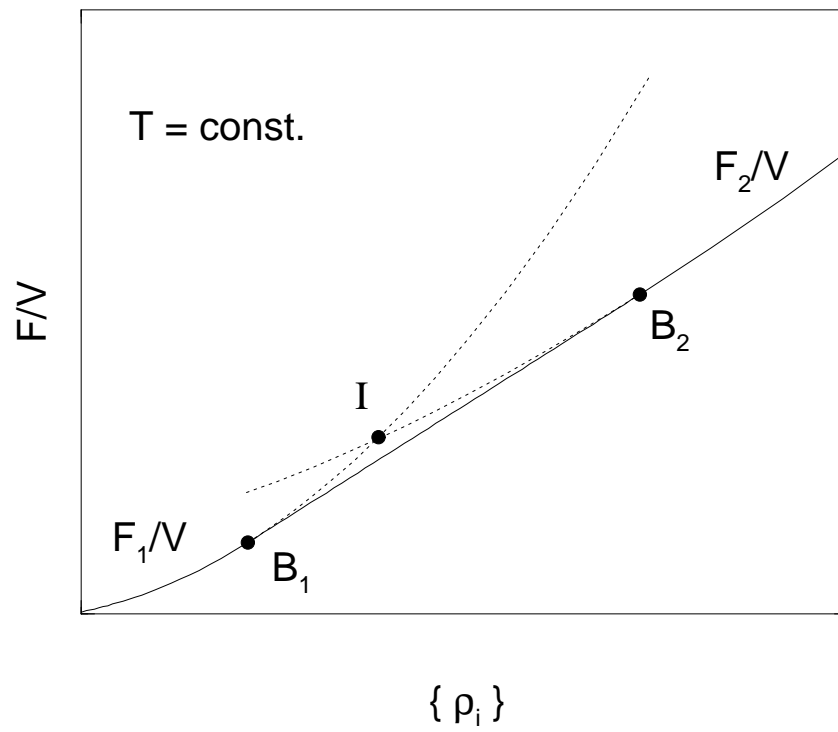
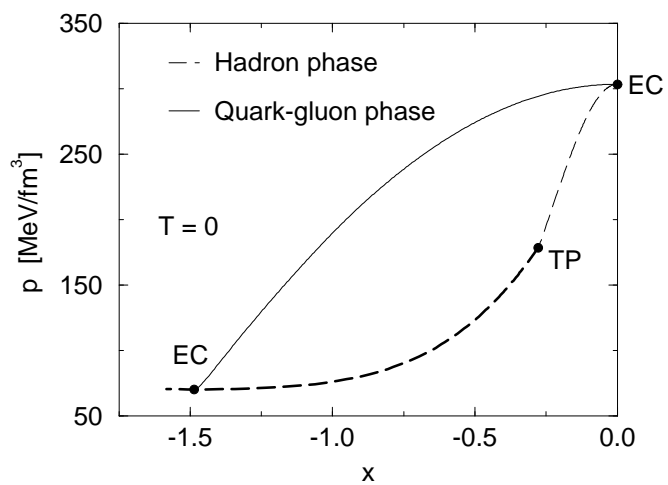
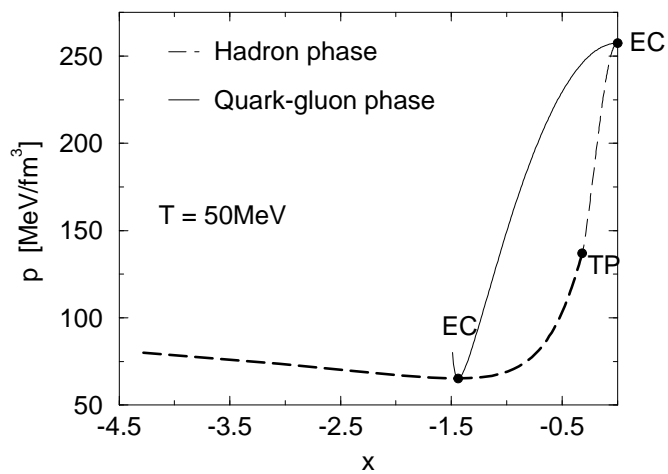


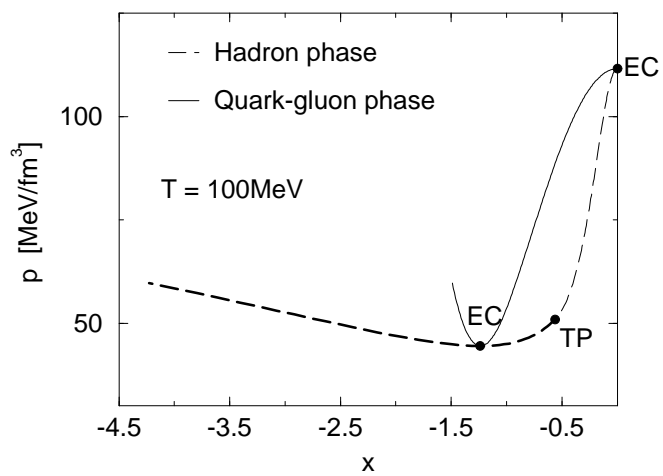
FIGURE 1



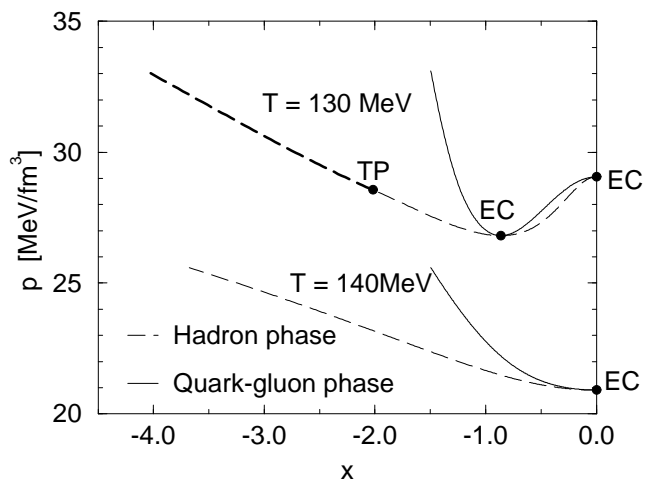
(a)



(b)



(c)



(d)

FIGURE 2

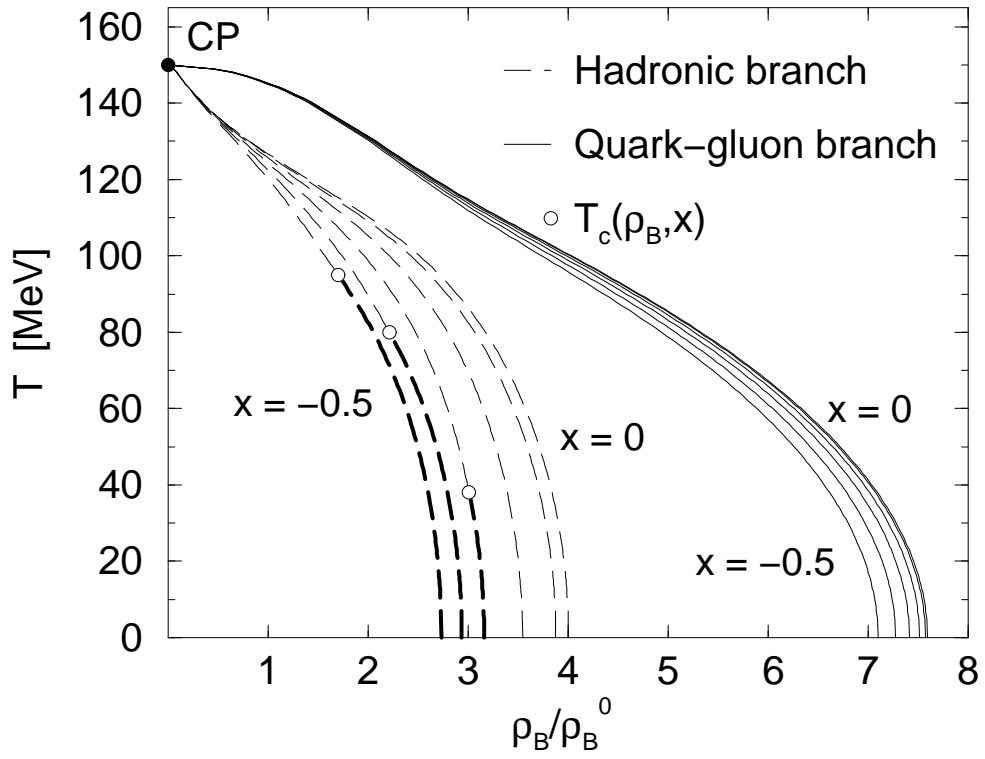


FIGURE 3

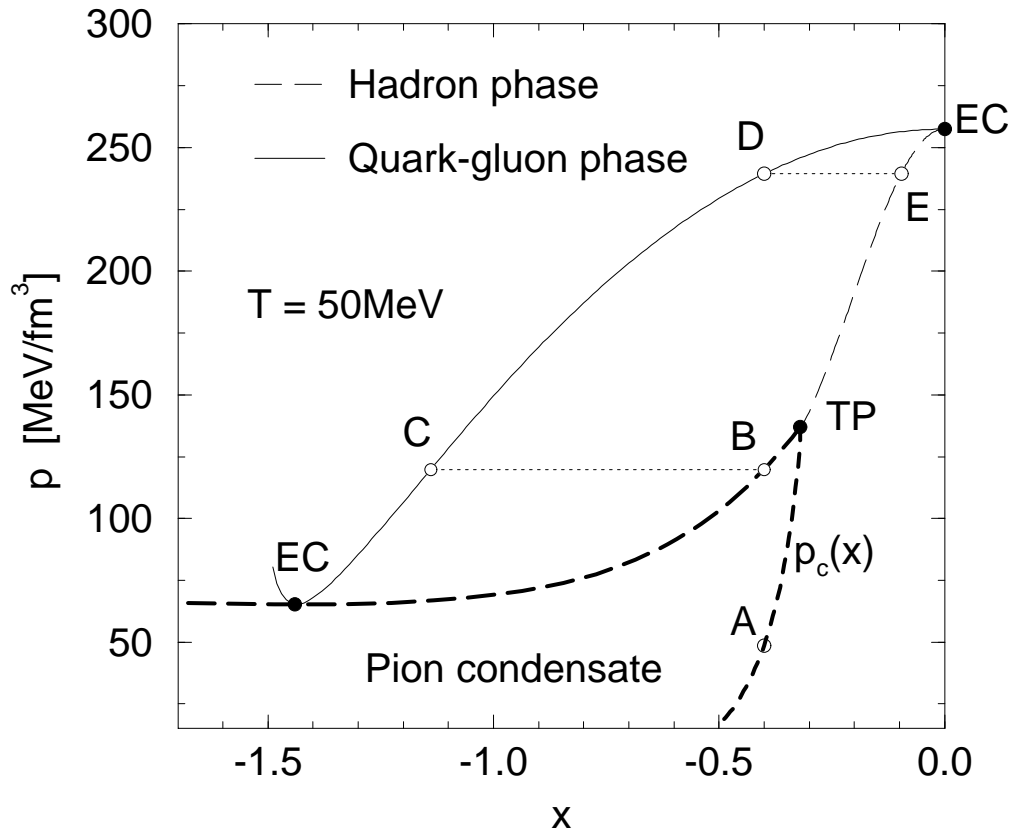


FIGURE 4 (a)

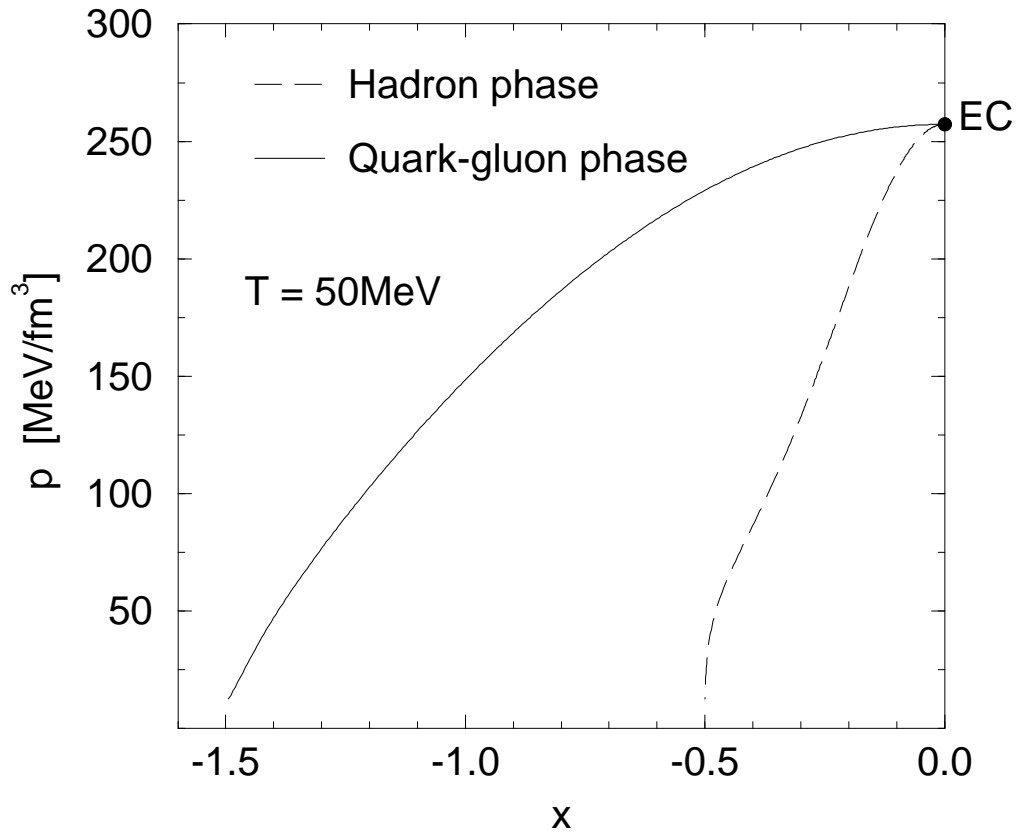


FIGURE 4 (b)

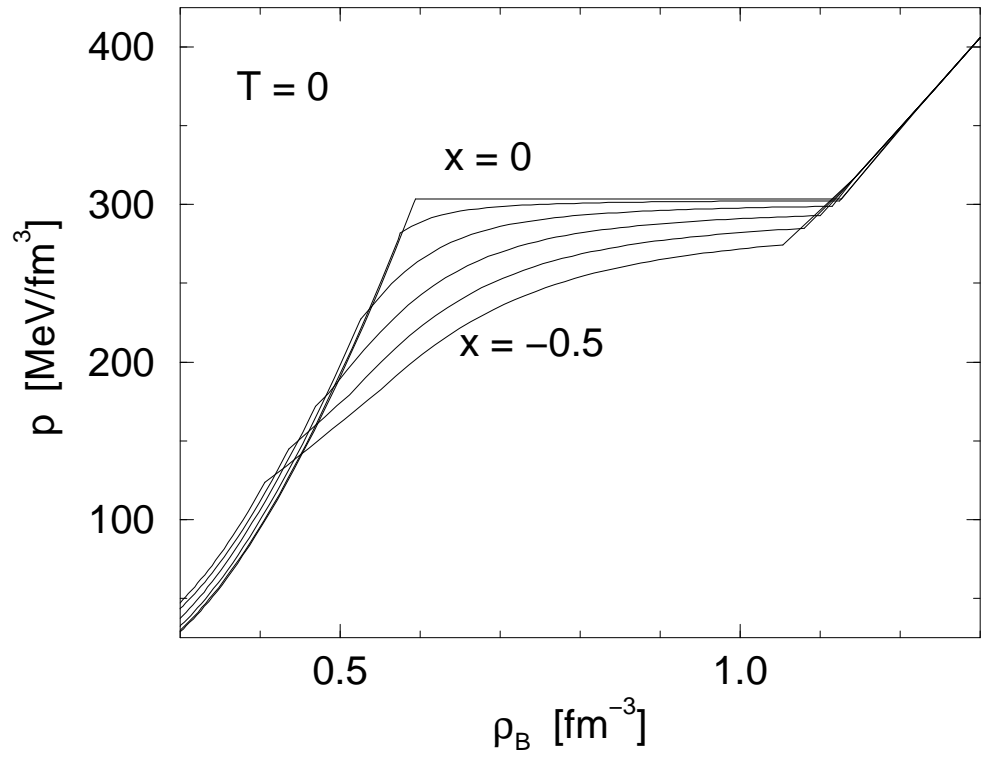


FIGURE 5 (a)

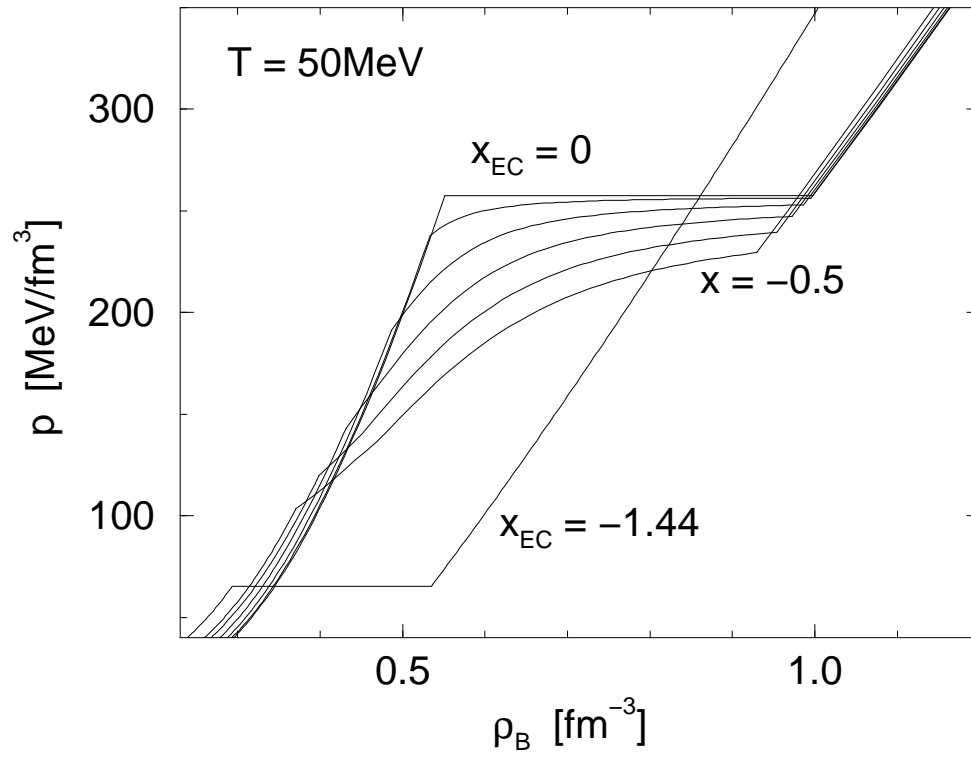


FIGURE 5 (b)

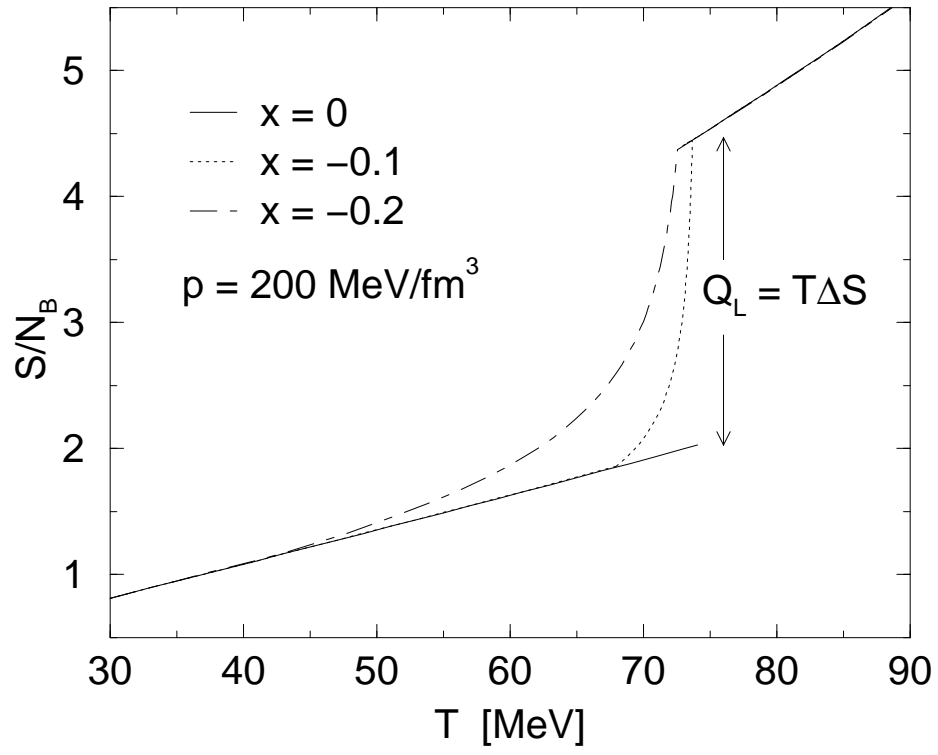


FIGURE 6

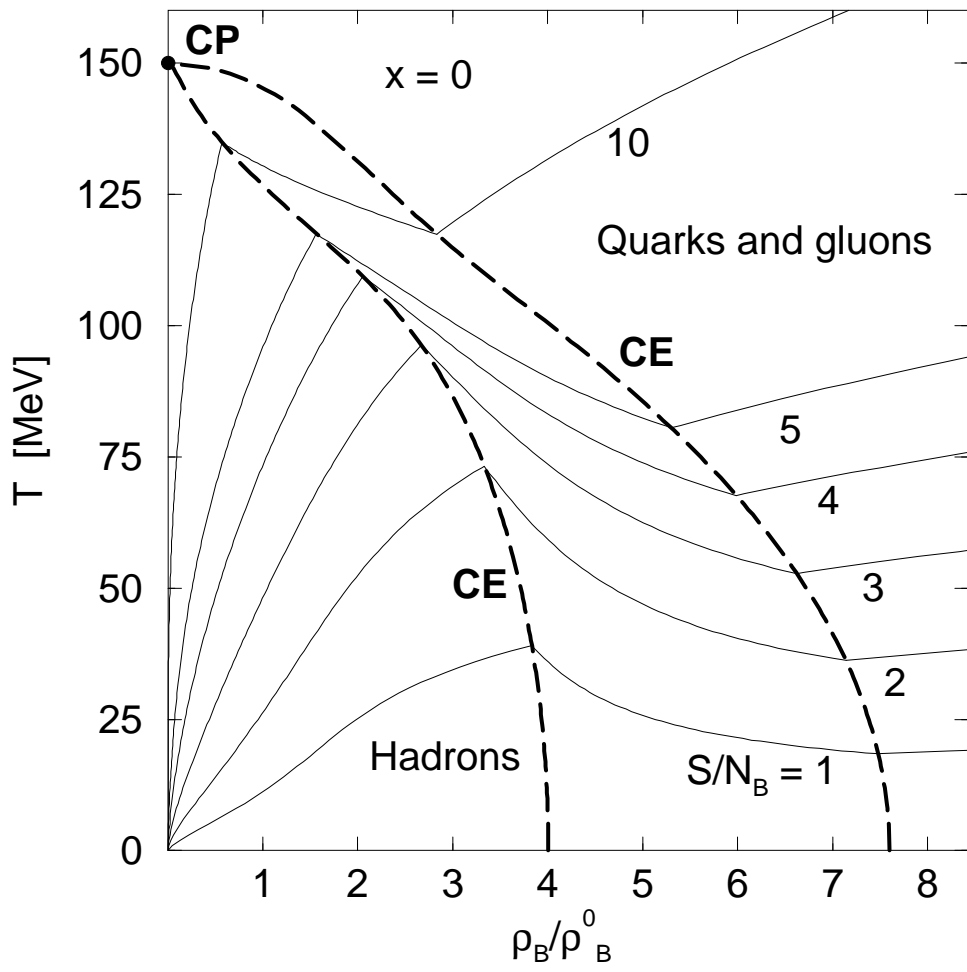


FIGURE 7(a)

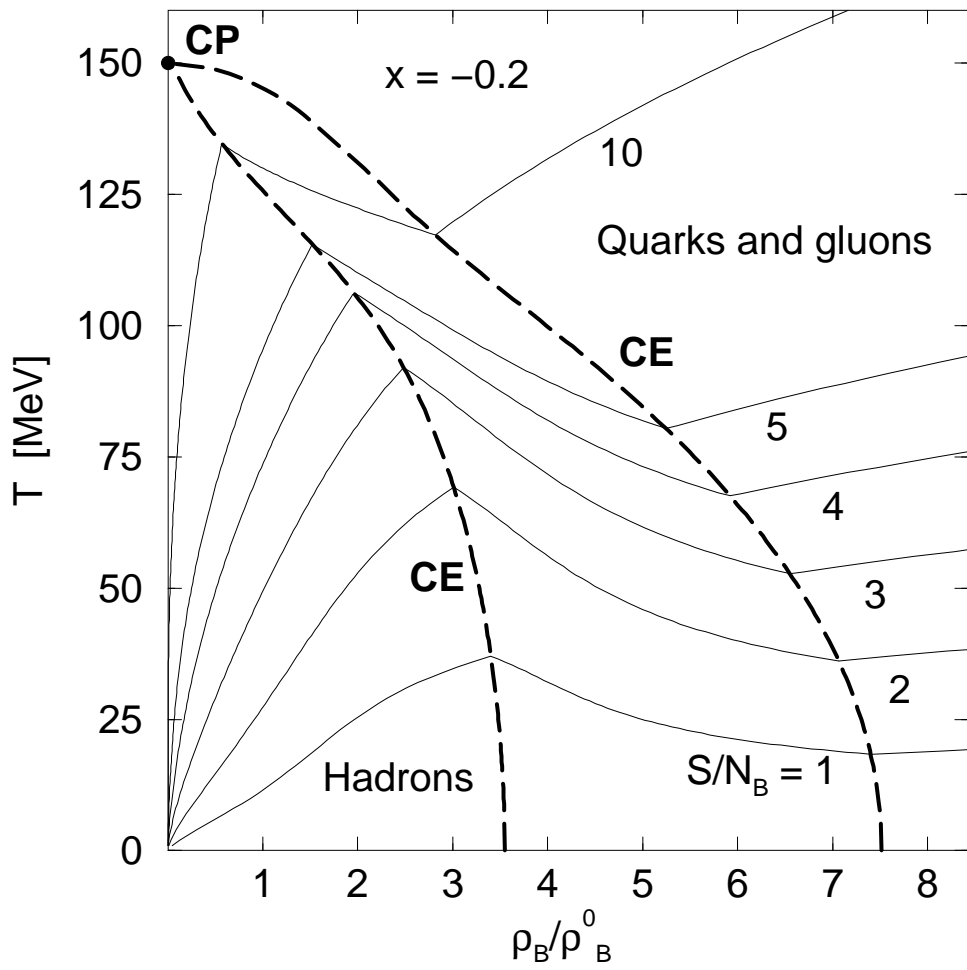


FIGURE 7(b)

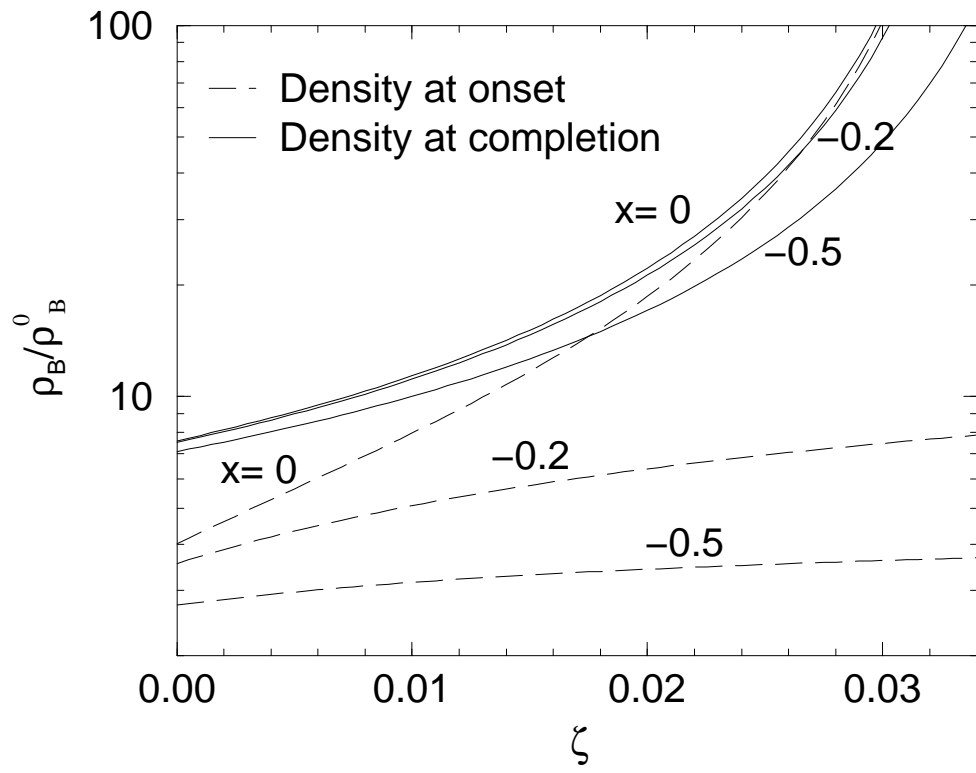


FIGURE 8